Anatomically modern human in Southeast Asia (Laos) by 46 ka

Fabrice Demeter[a,b,1], Laura L. Shackelford[c,1], Anne-Marie Bacon[d], Philippe Duringer[e], Kira Westaway[f], Thongsa Sayavongkhamdy[g], José Braga[b], Phonephanh Sichanthongtip[g], Phimmasaeng Khamdalavong[g], Jean-Luc Ponche[h], Hong Wang[i], Craig Lundstrom[j], Elise Patole-Edoumba[k], and Anne-Marie Karpoff[l]

[a]Department Homme Nature Société (HNS), National Museum of Natural History, Unité Mixte de Recherche (UMR) 7206/Unité Scientifique du Muséum (USM) 104, 75005 Paris France; [b]Formation de Recherche en Evolution (FRE) 2960 Anthropobiology Laboratory, Université Paul-Sabatier (UPS) Toulouse 3, 31000 Toulouse France; [c]Department of Anthropology, [i]Illinois State Geological Survey, Prairie Research Institute, and [j]Department of Geology, University of Illinois at Urbana–Champaign, Urbana, IL 61801; [d]Centre National de la Recherche Scientifique (CNRS) Unité Propre de Recherche (UPR) 2147, 75014 Paris France; [e]Institut de Géologie, Université de Strasbourg (UDS), Ecole et Observatoire des Sciences de la Terre (EOST), Institut de Physique du Globe de Starsbourg (IPGS), Centre National de la Recherche Scientifique (CNRS) Unité mixte de Recherche (UMR) 7516, 67084 Strasbourg Cedex, France; [f]Department of Environment and Geography, Macquarie University, NSW 2109, Sydney Australia; [g]Department of National Heritage, Ministry of Information and Culture, Vientiane Lao People's Democratic Republic; [h]LMSPC, UMR 7515 CNRS, F-67084 Strasbourg Cedex France; [k]DCP, C2RMF, 75001 Paris, France; and [l]Institut de Géologie, UDS, EOST, IPGS, CNRS/UDS UMR 7516, 67084 Strasbourg Cedex France

Edited by Erik Trinkaus, Washington University, St. Louis, MO, and approved July 23, 2012 (received for review May 14, 2012)

Uncertainties surround the timing of modern human emergence and occupation in East and Southeast Asia. Although genetic and archeological data indicate a rapid migration out of Africa and into Southeast Asia by at least 60 ka, mainland Southeast Asia is notable for its absence of fossil evidence for early modern human occupation. Here we report on a modern human cranium from Tam Pa Ling, Laos, which was recovered from a secure stratigraphic context. Radiocarbon and luminescence dating of the surrounding sediments provide a minimum age of 51–46 ka, and direct U-dating of the bone indicates a maximum age of ∼63 ka. The cranium has a derived modern human morphology in features of the frontal, occipital, maxillae, and dentition. It is also differentiated from western Eurasian archaic humans in aspects of its temporal, occipital, and dental morphology. In the context of an increasingly documented archaic–modern morphological mosaic among the earliest modern humans in western Eurasia, Tam Pa Ling establishes a definitively modern population in Southeast Asia at ∼50 ka cal BP. As such, it provides the earliest skeletal evidence for fully modern humans in mainland Southeast Asia.

human migrations | eastern Eurasia

Current paleontological evidence indicates that in the western Old World the initial appearance of anatomically modern humans occurred in eastern equatorial Africa 200–150 ka. This emergence was followed by a brief expansion into extreme southwestern Asia 120–90 ka and the complete establishment of modern humans and disappearance of late archaic humans by 50–40 ka (1, 2). Details of the process remain unclear, but the general framework has become robust. In the eastern Old World, the relevant data are far less complete and have been beset by difficulties in dating some of the purportedly early modern human remains (3, 4). Alternative attempts to date the spread of modern human morphology into eastern Eurasia either inappropriately equate technology with human biology (5–8) or use molecular clocks of unknown precision applied to extant human genetic data (9–11). The spread of modern human morphology into eastern Eurasia can only be documented by the discovery, dating, and morphological analysis of relevant Late Pleistocene human remains.

The most recent late archaic human fossils from eastern Eurasia are considered to be the Xujiayao craniofacial remains, dated to 125–100 ka, with the Maba 1 cranium being slightly older (3, 12–14). Possibly the oldest eastern Eurasian early modern human is currently a partial mandible from Zhirendong, southern China, securely dated to ∼100 ka (15). It exhibits a distinctive modern human anterior mandibular symphysis, despite corporeal robustness, but it provides little other morphological information. The next oldest securely dated specimen is the partial skeleton from Tianyuandong, northern China at ∼40 ka (16, 17). A partial cranium from Laibin, southern China (18) and the young adult Niah 1 cranium (the "Deep Skull") from Sarawak (19) are likely of similar age, although a U-series age estimate on the Niah 1 cranium suggests a slightly younger date. The partial skeleton from Liujiang and the Ziyang cranium might be as old, but there are uncertainties in their associations with dated materials (3, 4, 13, 20–22). In the Philippines, a modern human frontal bone from Tabon Cave is dated to 16.5 ka. More recently discovered remains from the site are directly dated to 24–58 ka, but these bones are nondiagnostic with respect to their modernity (23). Uncertainties also surround the ages of the earliest Australian human remains, even though humans were present in Australia more than 40 ka (24). The oldest modern human remains from South Asia, at Fa Hein in Sri Lanka, are modestly younger at ∼36 ka (25, 26). Early Holocene (14.3–11.5 ka) remains from southern China that were recently described as unique in their mixture of modern and archaic features (27) show common morphological features with Holocene human populations, notably in northern Indochinese provinces (28).

In this context, therefore, little is known of the eastern Eurasian human populations between ∼120 and 40 ka. A partial cranium of an early modern human from Tam Pa Ling (TPL), northern Laos, which was discovered in 2009, greatly contributes to this paleontological gap in the Late Pleistocene of Southeast Asia. Its suite of diagnostic modern human morphological features, secure stratigraphic context, and reliable dating are central to our understanding of the establishment and spread of early modern human biology in the region.

Context and Dating

TPL (Cave of the Monkeys) is located in Huà Pan Province, Laos, ∼260 km NNE of Vientiane (20° 12′ 31.4″ N, 103 ° 24′ 35.2″ E) (Fig. 1 and *SI Appendix*, Fig. S1). It occupies what is currently the top of the Pa Hang Mountain 1,170 m above sea level. The landscape consists of tower karsts derived from the dissolution of Upper Triassic limestone beds, with a dense network of caves and galleries. Tam Pa Ling has one main chamber

Author contributions: F.D., L.L.S., and A.-M.B. designed research; F.D., L.L.S., A.-M.B., T.S., J.B., P.S., P.K., J.-L.P., and E.P.-E. performed research; F.D., L.L.S., P.D., K.W., J.B., H.W., C.L., and A.-M.K. analyzed data; and F.D., L.L.S., A.-M.B., P.D., K.W., H.W., C.L., and A.-M.K. wrote the paper.

The authors declare no conflict of interest.

This article is a PNAS Direct Submission.

[1]To whom correspondence may be addressed. E-mail: demeter@mnhn.fr or llshacke@illinois.edu.

This article contains supporting information online at www.pnas.org/lookup/suppl/doi:10.1073/pnas.1208104109/-/DCSupplemental.

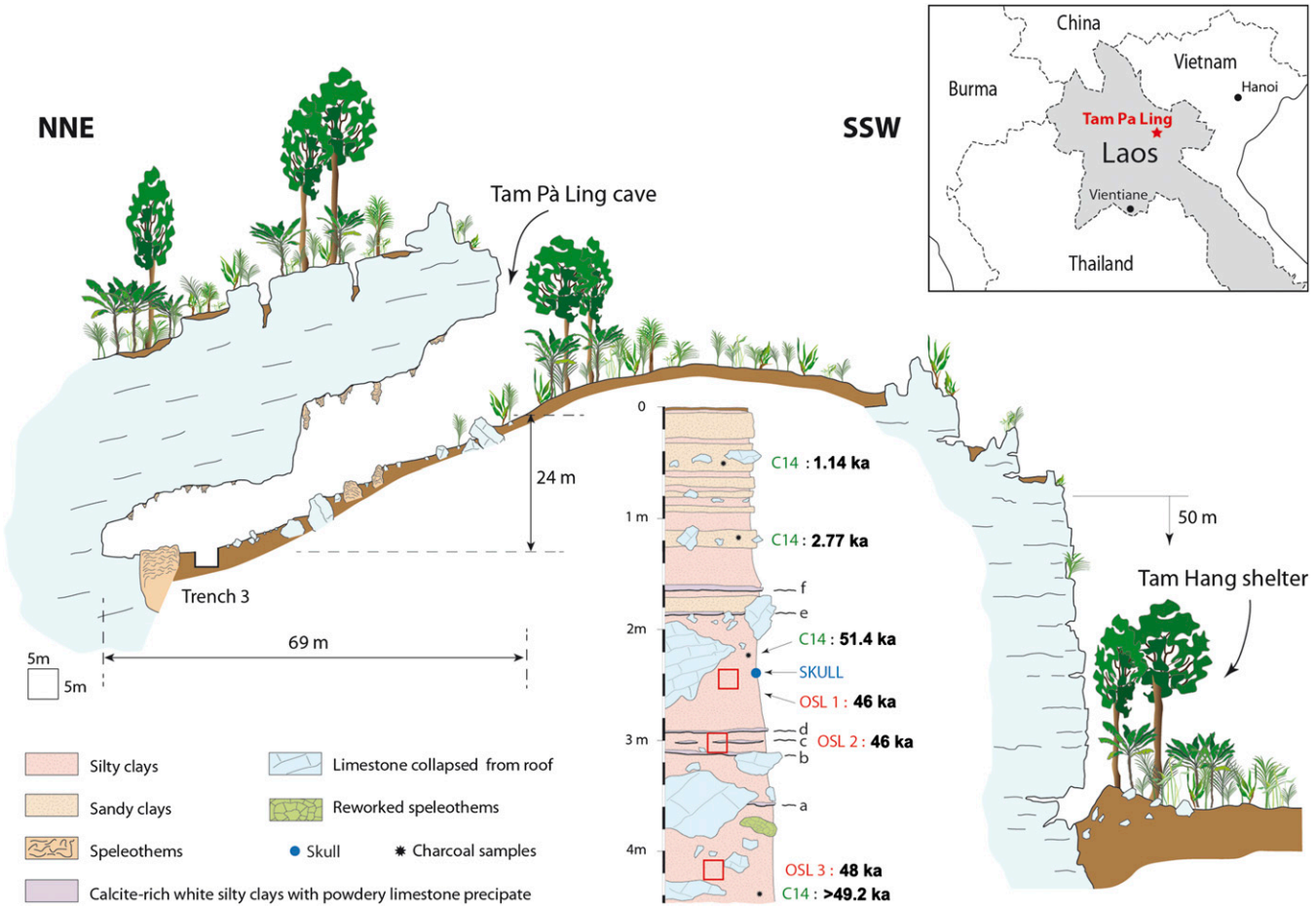

Fig. 1. Site of TPL, Laos. TPL is located on the upper plateau of the Pa Hang Mountain, with the Tam Hang rock shelter lying at the mountain's base. The 4-m stratigraphy shows the accumulation of sandy and silty clay layers punctuated by six powdery limestone precipitates (a–f) from the TPL trench. Provenance of the charcoals sampled for ^{14}C dating and soil sampled for OSL and TL dating is identified on the stratigraphy. TPL 1 was lying at a depth of 2.35 m. *Inset*: Location of TPL in Huà Pan Province, Laos.

(40 m width × 30 m length × 12 m height) with a south-facing entrance that is partially blocked by meter-sized limestone blocks from a roof collapse. Upon entering the cave, a steep, 65-m slope descends to the chamber floor. The 30-m length of the gallery is oriented in a north–south direction; its 40-m width is oriented in an approximate east–west direction. In 2008, three test pits were opened on the cave floor to examine stratigraphy and sedimentology: trenches 1 and 2 on the west side and trench 3 on the east side (*SI Appendix*, Fig. S2). In 2009 and 2010, the main excavation (trench 3) at the east end of the gallery was excavated to a maximum depth of 4.3 m (*SI Appendix*, Figs. S2 and S3). At a depth of 2.35 m, we recovered a partial human cranium, including the frontal, partial occipital, right parietal, and temporal, and maxillae with largely complete upper dentition (TPL 1; Fig. 2 and *SI Appendix*, Fig. S4). The association of the individual cranial remains within 30 cm^2 in situ and their articulation indicate that they are from a single individual. A small number of micromammal and reptile remains were recovered from the same layer, including fragmentary long bone shafts, vertebrae, and partial dentitions. No artifacts were found in the site, and there is no evidence of human occupation. The state of preservation and the absence of water-rolling evidence suggest that all faunal remains originated near the cave entrance and were carried into the cave via relatively slow, low-energy slopewash transport.

Sediments in the stratigraphic sequence of the excavation form a series of intercalated, clay-rich slopewash deposits that originated outside the south-facing entrance and were carried into the cave (Fig. 1). The layers alternate between sandy and silty clays and contain small limestone clasts and iron-oxides pisolites (Fig. 1 and *SI Appendix*, *SI Text*). The former are derived from the surrounding substratum, whereas the quartz, clays, and secondary iron oxides are derived from outside the cave. The clay composition (vermiculite and kaolinite associated with iron and aluminum oxides) indicates hydrolyzing leaching conditions that are characteristic of "ferralsols-nitisols" strongly weathered soil types, suggesting they were deposited during a humid, subtropical climate.

From the top of the section to a depth of ~2 m, brown sandy clays alternate with thin layers of silty clays. The lowest section of the deposit (from ~2 m to its base) is formed from continuous silty clays (Fig. 1 and *SI Appendix*, *SI Text* and Fig. S5). These clay-dominated cave infillings are punctuated by six white silty clays (Fig. 1 *A*–*F*) with concentrations of a powdery limestone reprecipitate, which can be followed without discontinuity across the excavation. There is no evidence in the excavated strata of bioturbation, postdepositional modifications, soft deformations, reworking, or mixing. Stratigraphy and sedimentation is consistent between the three trenches, and the individual laminae can be followed laterally across the chamber (*SI Appendix*, Figs. S5–S7).

Multiple dating techniques were used to constrain the age of TPL 1, including radiocarbon dating of charcoal and luminescence dating of sediments from the sedimentary column. Because the stratigraphic integrity of the site has been maintained despite periodic slopewash into the cave, these ages provide

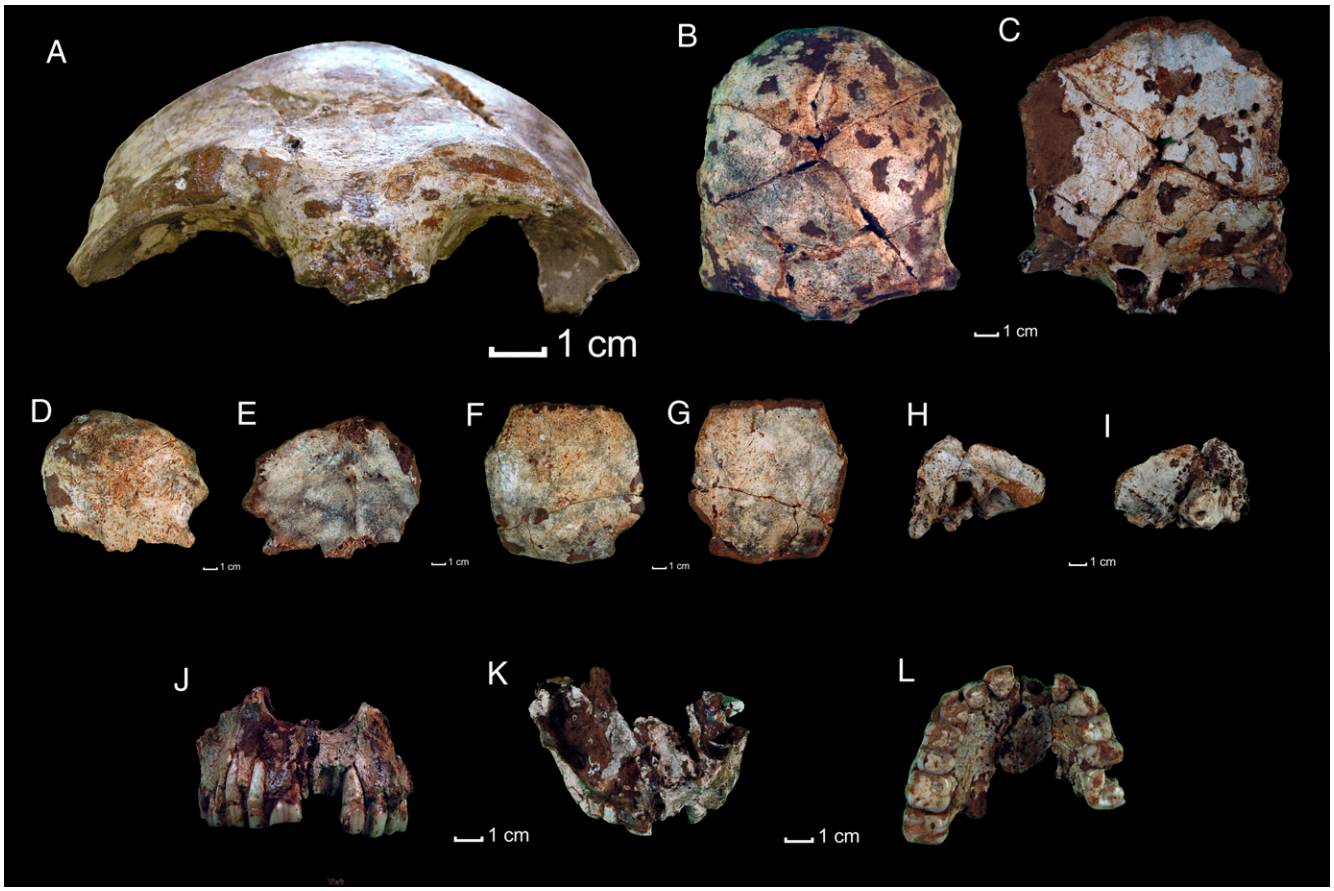

Fig. 2. Human fossil remains designated as TPL 1. (*A*) frontal bone in *norma facialis*; (*B*) frontal bone in in *norma verticalis*; (*C*) frontal bone in in *norma basilaris*; (*D*) occipital bone in *norma verticalis*; (*E*) occipital bone in *norma basilaris*; (*F*) right parietal bone in *norma verticalis*; (*G*) right parietal bone in *norma basilaris*; (*H*) left temporal bone with partial mastoid in *norma lateralis*, external; (*I*) left temporal bone with partial mastoid in *norma lateralis*, internal; (*J*) maxillae in *norma facialis*; (*K*) maxillae in *norma verticalis*; (*L*) maxillae in *norma basilaris*.

a minimum age for fossil deposition. A sample of the frontal bone of TPL 1 was directly dated by U-series.

Four charcoal samples were collected for radiocarbon dating (Fig. 1). Radiocarbon dating of charcoal in the sedimentary column from depths of 2.1 m and 4.3 m (Fig. 1) yielded ages of 56.5 ka cal BP (51.4 ^{14}C ka) and an infinite age of >54 ka cal BP (>49.2 ^{14}C ka), respectively (*SI Appendix*, Table S1). These AMS ^{14}C assays are used as a chronological indicator rather than a "true" burial age because they lie at the upper limits of ^{14}C dating, and the charcoal was not derived from in situ occupation deposits but was washed into the cave.

Sediment samples were dated using thermoluminescence (TL) and optically stimulated luminescence (OSL) techniques. Luminescence techniques measure the time at which sediments were last exposed to heat (TL) or sunlight (OSL). Naturally occurring minerals, such as quartz and feldspar, have a crystalline structure that can store energy. During burial, these minerals store a proportion of the energy that they receive from radiation in the surrounding sediment. This stored energy may be released (thus resetting the signal to zero) by heating or by exposure to sunlight, allowing the estimation of the time elapsed since the sediments that encased the fossil were buried (29, 30). Granitic quartz produces both red and UV emissions (31–34), allowing for red TL dating of the red emissions and UV OSL dating of single aliquots and single grains as an internal test of paleodose consistency.

Three associated silty clay sediment samples were collected at 2.35 m (Fig. 1, between e and d), 3.15 m (Fig. 1, between d and b), and 4.20 m (Fig. 1, below a) and constrained by TL and OSL applications. Single-aliquot regenerative dose OSL using UV emissions of single aliquots and single grains (35) and dual-aliquot protocol red TL using red emissions (36) produced a combined age of 46 ka and a basal age of 48 ka, with maximum ages of 50–51 and 57 ka, respectively (Table 1). When combined the results indicate that the fossils were buried no later than 46 ka and no earlier than 47–51 ka. Given that the fossils washed into the cave, the sedimentary burial occurred before 46 ka, making them of greater antiquity.

The stratigraphy shows a chronological hiatus in the upper part of the section, as shown in Fig. 1 at the levels indicated as "e" and "f." The age of the sediment column is dated to 46 ka (OSL) and 51.4 ^{14}C ka cal BP (AMS ^{14}C) below "e" and to 2.77 ka cal BP (AMS^{14}C) above "f." This gap could have several origins (*SI Appendix*, *SI Text*), but owing to the lack of an erosion contact between the lower and upper parts of the section, it most likely indicates a change in the cave entrance morphology (open or closed) that conditioned the slopewash activity.

The teeth of the TPL 1 are fragile and have been treated with preservative, so a portion of the frontal bone was sampled for U/Th dating. The sample was of good composition and was dissolved in 8N HNO3. Isotopic tracers ^{229}Th and ^{236}U were added. When measuring the isotope ratios that were <<1% (2s) with a negligible age correction for an assumed bulk earth detritus, a 10% error was assigned to the age. TPL 1 is directly dated by U/Th to 63.6 ± 6 ka (*SI Appendix*, Table S2).

This age range for the TPL 1 human remains indicates they are modestly older than the Tianyuandong and Niah Cave remains, with a minimum secured age of 46 ka and a maximum age of ~63 ka. Only the Zhirendong fossils are older, and they

Table 1. UV OSL and red TL dating of sediments from TPL: Dose rate data, equivalent doses, and ages

Sample code*	Sample depth (m)	Radionuclide activities (Bq kg^{-1})†						Field γ dose rate‡ (Gy ka^{-1})	Cosmic-ray dose rate§ (Gy ka^{-1})	Water content¶ (%)	Total dose rate‖ (Gy ka^{-1})	Signal	Equivalent dose**,†† (Gy)	Age†††,‡‡,§§ (ka)
		^{238}U	^{226}Ra	^{210}Pb	^{228}Ra	^{228}Th	^{40}K							
TPL 1	2.35–2.55	81.0 ± 7.0	48.6 ± 1.3	55.3 ± 6.0	80.6 ± 2.8	83.0 ± 2.2	357 ± 16	1.205 ± 0.042	0.019	42/40 ± 5	2.60 ± 0.16	UV_{SA}	127 ± 9	49 ± 5
											2.53 ± 0.15	UV_{SG}	116 ± 7	46 ± 4
											2.60 ± 0.16	R	137 ± 26	52 ± 10
											2.60 ± 0.16	R_{MUL}	130 ± 29	50 ± 12
TPL 2	3.15–3.35	57.1 ± 7.4	50.2 ± 1.4	58.5 ± 7.2	90.5 ± 3.0	91.3 ± 2.4	364 ± 15	1.292 ± 0.050	0.019	39/40 ± 5	2.68 ± 0.18	UV_{SA}	126 ± 11	47 ± 5
											2.61 ± 0.18	UV_{SG}	119 ± 10	46 ± 5
											2.68 ± 0.18	R	144 ± 43	53 ± 16
											2.68 ± 0.18	R_{MUL}	136 ± 40	51 ± 15
TPL 3	4.20–4.40	56.4 ± 7.6	45.5 ± 1.4	47.4 ± 6.6	81.8 ± 3.0	82.4 ± 2.3	460 ± 18	1.122 ± 0.038	0.018	59/45 ± 5	2.70 ± 0.18	UV_{SA}	135 ± 11	50 ± 6
											2.63 ± 0.17	UV_{SG}	126 ± 10	48 ± 5
											2.70 ± 0.18	R	165 ± 70	61 ± 26
											2.70 ± 0.18	R_{MUL}	154 ± 33	57 ± 13

*Samples processed using the 90- to 125-μm size fraction (single aliquots) and the 180- to 212-μm size fraction (single grains).
†Concentrations determined from high-resolution γ spectrometry measurements of dried and powdered sediment samples.
‡Determined from U, Th, and K concentrations measured using a portable γ-ray spectrometer at field water content.
§Time-averaged cosmic-ray dose rates (for dry samples), each assigned an uncertainty of ±10%.
¶Field/time-averaged water contents expressed as (mass of water/mass of dry sample) × 100. The latter values were used to calculate the total dose rates and OSL/TL ages.
‖Mean ± total (1σ) uncertainty calculated as the quadratic sum of the random and systematic uncertainties. An internal dose rate of 0.03 Gy ka^{-1} is also included. An additional 6% was included in the error to account for the uncertainty in the dose rate estimation due to the disequilibrium. The difference in dose rates between the single-grain UV, multiple-grain red TL, and single-grain UV results relates to the differing dose attenuation in 100- and 200-μm grains.
**Paleodoses include a ±2% systematic uncertainty associated with laboratory β-source calibrations.
††UV_{SA}, UV OSL signal measured using small (0.5-mm) single aliquots. On average, 48 discs were run for each sample, with a 13% rejection rate (8 discs were rejected out of a possible 48 per sample), with the D_e derived from a minimum age model (MAM); UV_{SG}, UV OSL signal measured using single grains of quartz. On average, 1,200 grains were analyzed for each sample, with 6–10% of the grains emitting an acceptable luminescence signal, with the D_e derived from a MAM; R, easy-to-bleach red signal. Only two large aliquots were analyzed per sample; R_{MUL}, multiple red TL measurements to assess variability between aliquots. Twelve aliquots were measured, with similar rejection criteria and a MAM applied.
‡‡Uncertainties at 68% confidence interval.
§§Locations of samples TPL 1–3 can be seen in Fig. 1.

preserve limited anatomy of the mandible and combine archaic and modern human aspects.

TPL 1 Human Remains

The TPL 1 human remains include the frontal, partial occipital, right parietal, and temporal, and right and left maxillae with largely complete dentition (right I2–M2 and left I2–M1) (Fig. 2). A distal interproximal facet on the right M^2 indicates that the M^3 was in occlusion, and hence the individual was mature. Minimal wear on the remaining molars suggests a young adult (*SI Appendix*, Table S4).

The most distinctive aspect of TPL 1 is the complete absence of a supraorbital torus on the largely complete frontal bone (Fig. 2*A*). The superciliary arches are relatively prominent, beginning adjacent to nasion medially and arching over the medial two-thirds of the orbits. There are lateral trigones above the lateral third of each orbit, bounded laterally by the temporal lines and anteroinferiorly by distinct and angular orbital margins. Although fusion of these elements, and hence a supraorbital torus, is present among some modern humans, none of the nonmodern members of the genus *Homo* exhibit the distinct separation of these elements and hence the absence of a supraorbital torus (37, 38). The TPL 1 frontal bone also has a minimal postorbital constriction (Fig. 2 *A*–*C*). A posterior view of the reconstructed TPL 1 partial calotte shows a clear angulation at the parietal eminences with a rounded sagittal suture that gives the skull a shape described by Doboş et al. (39) as "en fesses de cheval" (*SI Appendix*, Fig. S8). This is characteristic of modern humans and distinguishes TPL 1 from the East Asian late archaic remains from Maba and Xujiayao, whose parietals are rounded.

The preserved occipital squama includes the superior nuchal plane and most of the occipital plane (Fig. 2 *D* and *E*). There is an external occipital protuberance at inion that lies immediately inferior to a small, triangular depression on the occipital plane. There is no suprainiac fossa, as is found in western Eurasian Neandertals, and there is no transverse occipital (nuchal) torus, as seen in pan-Eurasian archaic humans (including the late archaic Xujiayao 6 and 12) (3, 40, 41). In addition, the right transverse sinus crosses the lambdoid suture, and the parietal bone above asterion, before descending into the sigmoid sinus, which is the more common modern human pattern.

The right temporal bone fragment includes the petrous, tympanic, and partial mastoid regions, including the anterolateral mastoid process (Fig. 2 *H* and *I*). From the root of the zygomatic process, the suprameatal crest runs horizontally and superior to the external auditory porous and continues as a weakly developed supramastoid crest. The external auditory porous is elliptical, with its long axis oriented anterosuperiorly to posteroinferiorly. In these features TPL 1 contrasts with the configurations seen in most Neandertals, as well as in most East Asian Middle Pleistocene *Homo erectus* (42), and resembles the patterns evident globally in early and recent modern humans (43, 44). However, these configurations are also present in the late archaic Xujiayao 15 temporal bone (3) and may therefore only serve to distinguish TPL 1 from Neandertals and Middle Pleistocene humans.

In addition to the alveoli and partial dentition, the right maxilla preserves part of the maxillary sinus and the inferior frontal process; the left maxilla maintains a small portion of the maxillary sinus and the partial nasal floor (Fig. 2 *J*–*L*). The nasal aperture is bounded anteroinferiorly by a moderate nasal sill and modest anterior nasal spines. The level nasal floor is the pattern more frequently present among early and recent modern humans (45). A recent study of eastern Eurasian Pleistocene *Homo* reinforces this pattern, with available early modern human remains having level nasal floors and preserved archaic human fossils demonstrating bilevel or sloping nasal floors (46). These results indicate that it is not only Neandertals but archaic humans across the Old World that have the distinctive bilevel nasal floor, and both European and Asian early modern humans are characterized by the level floor seen in TPL 1. The nasal aperture of TPL 1 is relatively wide for a European early modern human, although it is normal relative to other Asian early modern humans; it does not approach

Table 2. Buccolingual crown diameters for maxillary dentition and nasal breadth of TPL 1 and comparative samples

Tooth position	TPL 1	W-LA	E-LA	MPMH	W-UP	E-LP
I1	7.4 (R)	8.1 ± 0.59 (35)	7.7 ± 1.13 (3)	8.2 ± 0.50 (12)	7.7 ± 0.49 (41)	7.4 ± 1.10 (14)
I2	7.5 (R) 6.9 (L)	8.1 ± 0.52 (37)	6.0 (1)	7.5 ± 0.58 (11)	6.9 ± 0.59 (42)	7.82 ± 1.07 (5)
C	10.6 (R) 9.2 (L)	9.6 ± 0.58 (33)	10.1 ± 0.50 (2)	9.2 ± 0.78 (10)	9.0 ± 0.89 (46)	8.1 ± 0.75 (9)
P3	11.6 (R) 10.1 (L)	10.5 ± 0.54 (33)	11.5 ± 0.89 (5)	10.4 ± 0.36 (9)	9.8 ± 0.68 (51)	8.1 ± 1.48 (13)
P4	10.8 (R) 11.2 (L)	10.0 ± 0.61 (30)	—	10.1 ± 0.75 (12)	9.8 ± 0.63 (46)	7.1 ± 1.16 (9)
M1	12.7 (R)	12.0 ± 0.75 (44)	13.0 ± 1.37 (4)	12.1 ± 0.64 (19)	12.2 ± 0.78 (75)	11.6 ± 1.20 (16)
M2	13.3 (R)	12.2 ± 0.95 (35)	13.7 (1)	12.1 ± 0.70 (10)	12.3 ± 0.95 (72)	11.2 ± 1.60 (14)
Nasal breadth (M-54)	28.0	32.0 ± 3.3 (18)	28.5 (1)	31.2 ± 1.2 (5)	25.8 ± 2.1 (26)	26.7 ± 2.7 (6)

All measurements in millimeters. Data given as mean ± SD (*n*). Samples are as follows: W-LA, western Eurasian late archaic humans; E-LA, eastern Eurasian late archaic humans; MPMH, Middle Paleolithic modern humans; W-UP, western Eurasian Upper Paleolithic humans; E-LP, eastern Eurasian Late Pleistocene humans. Additional information on sample composition can be found in *SI Appendix*. L, left; R, right; —, no data available.

the high values evident in archaic *Homo* or the southwestern Asian Middle Paleolithic modern humans (Table 2).

The TPL 1 maxillary dentition includes the right I1 to M2 and the left I2 to M1. All of the teeth are cracked and fissured except the right I1 and P3–M2, and wear obscures most of the occlusal morphology (Table 2 and *SI Appendix*, Fig. S4). Moreover, even though a series of late archaic vs. early modern human dental morphological differences have been identified for western Eurasia (47), these purported Neandertal apomorphies seem to be absent in eastern Eurasia (48). As such, it is unclear what might constitute a derived East Asian modern human dental pattern. The TPL 1 dentition, to the extent that can be determined given the extensive wear, has labial convexity of the I1 and I2s and a small canine lingual tubercle. There are four cusps on the M1 and M2 with a reduced hypocone on the M2, peripheral placement of the molar cusps, no skewing of the occlusal outline, and absence of a Carabelli's cusp.

At the same time, however, the dentition of TPL 1 follows the pattern seen in early modern humans relative to at least western late archaic humans: small anterior teeth despite little reduction in postcanine tooth size (49, 50). The buccolingual diameters of the TPL 1 I1 to C are among the smallest of those for the late archaic and Middle Paleolithic modern humans, but its M1 and especially P4 and M2 crown breadths are among the largest of those from the Late Pleistocene (Table 2). Of particular relevance, when the summed anterior crown breadths are plotted against the summed posterior ones, there is almost complete separation of the archaic vs. Upper Paleolithic samples, and TPL 1 falls among the early modern humans with relatively small anterior teeth (*SI Appendix*, Fig. S9). Comparative maxillary data are only available for eastern Eurasian Late Pleistocene humans from Tam Hang, Laos, which demonstrate relatively small anterior and posterior dentition. The early modern Tianyuandong 1 mandibular dentition shows relative anterior dental reduction, although not as pronounced as in TPL 1 (17).

Discussion

From these considerations of the TPL 1 morphology, it is evident that the cranium exhibits a suite of derived morphological features of modern humans, especially in a Late Pleistocene context. Foremost is the complete absence of a supraorbital torus. This is joined by the small postorbital constriction, the absence of a transverse occipital torus, the presence of a distinct external occipital protuberance, and the anterior-to-posterior dental proportions. Other features distinguish it from western Eurasian late archaic humans (Neandertals)—most notably its temporal morphology, the absence of a suprainiac fossa, and aspects of dental occlusal morphology—but they do not seem to separate it from eastern Eurasian late archaic humans. These morphological aspects, in the context of what some researchers consider an increasingly documented archaic–modern morphological mosaic among the earliest modern humans in the western Old World, indicate that the TPL 1 cranium represents an early modern human population in Southeast Asia.

Mainland Southeast Asia is notable for its absence of fossil evidence for early human occupation, mainly due to taphonomic issues in a warm and wet climate. Thus, the secure stratigraphic context and dating of the sedimentary column to 51–46 ka, combined with a possible maximum age of ~63 ka, makes TPL 1 the earliest well-dated human fossil east of the Jordan Valley that exhibits a suite of distinctive modern human morphological features. If the Zhiren 3 anterior mandible represents an early modern human, according to its anterior symphyseal morphology despite its corporeal hypertrophy, TPL 1 helps to fill in the chronological gap that currently exists in the early modern human paleontological record of this southeast portion of Asia. If Zhiren 3 is, alternatively, considered to be more ambiguous in its modern human affinities, then TPL 1 provides the earliest secure evidence for fully modern human morphology in the region. As such, it would provide a minimal baseline for the spread of modern human biology in eastern Eurasia, including the penecontemporaneous dispersal of humans into Australasia.

This temporal baseline for occupation of eastern Eurasia corresponds to the timing of the earliest dispersal events into Southeast Asia using genetic data. Inferences from nuclear (51), Y chromosome (52), and mitochondrial genome (53) data support an early migration of modern humans out of Africa and into Southeast Asia using a southern route by at least 60 ka. Patterns of genetic variation in recent human populations (11, 54, 55) recognize Southeast Asia as an important source for the peopling of East Asia and Australasia via a rapid, early settlement. In addition, the focus of hypotheses regarding early modern human migration in the region has concentrated on island and coastal regions. The fossil evidence presented here suggests that Pleistocene modern humans may have followed inland migration routes or used multiple migratory paths.

Materials and Methods

A comparative assessment of the TPL 1 human remains was performed using distributions of linear measurements. Standard craniometrics were taken whenever possible given preservation of relevant bones and landmarks, primarily on the frontal bone and dentition. Estimates of buccolingual and mesiodistal diameters for the dentition of TPL 1 are provided in *SI Appendix*, Table S4. The dentition was cracked and fragmented, allowing for the possible expansion of some teeth from sediment-filled fissures, most notably

the right C, P3, and P4. The mesiodistal dimensions of all preserved dentition are reduced by interproximal tooth wear. Given this attrition, only buccolingual diameters were used to make comparisons of proportions along the dental arcade between paleontological samples.

The age of TPL 1 suggests that it was contemporaneous with archaic humans in the western Old World. Its features, however, are relatively gracile and lack many of the characteristic features of the European and Near Eastern Neandertals. Given the age and morphology of the fossil, it is appropriate to evaluate TPL 1 relative to these samples. Also of interest is the similarity or difference between TPL 1 and other East and Southeast Asian archaic and modern human fossils, particularly the Chinese specimens of Xujiayao dated to 125–100 ka cal BP, Zhirendong dated to ~100 ka cal BP, Tianyuandong dated to ~40 ka cal BP, and those from the nearby site of Tam Hang, Laos, dated to ~16 ka cal BP.

The TPL 1 remains were compared principally with five paleontological samples: western Eurasian late archaic humans (Neandertals, all Late Pleistocene), eastern Eurasian late archaic humans (terminal Middle to early Late Pleistocene, which most workers may group as Neandertals), Middle Paleolithic modern humans, western Eurasian Upper Paleolithic humans, and eastern Eurasian Late Pleistocene humans. The eastern Eurasian Late Pleistocene human sample is more problematic becaues there are uncertainties regarding the taxonomic status, stratigraphic association, and/or dating of some of these fossils. To maximize these data, East and Southeast Asian fossils that are accepted as modern human are included despite their age because it can be assumed that no speciation events are observable within the sample.

Samples were evaluated for differences in morphological traits of the frontal bone and dentition using model II ANOVA with post hoc Bonferroni tests for multiple comparisons. Comparative data were provided by E. Trinkaus (St. Louis, MO) and S. Athreya (Texas). Results for morphological comparisons are given in Table 2 and *SI Appendix*, Fig. S9 and Tables S3 and S4.

ACKNOWLEDGMENTS. We thank the authorities of Vientong village (Hua Pan Province) for their support since 2003. We also thank Erik Trinkaus for his advice and assistance in preparing this manuscript, as well as for providing comparative data; Sheela Athreya for providing frontal bone data; Prof. Mike Morwood for helpful discussions and advice on an earlier version of this manuscript; Prof. C. Marsault and I. Laurenson for providing us with scanner facilities (Radiology Department, Hopital Tenon, Paris); and Daniel Fouchier Unité Propre de Recherche (UPR) 2147 and Annie Bouzheghaia (University Louis Pasteur) for drawings and graphics. This work is supported by the French Ministry of Foreign Affairs, the Ministry of Culture and Information of LAO People's Democratic Republic, University of Illinois at Urbana-Champaign, UPR2147 (Centre National de la Recherche Scientifique), Unité Mixte de Recherche (UMR) 7206 (Museum national d'Histoire naturelle, Paris), Formation de recherche en Evolution (FRE) 2960 (Université Paul Sabatier), and the L.S.B. Leakey Foundation. Chronological aspects of this research were partially funded by Australian Research Council Grants DP1093049 to (K.W.) and LE100100094 (to Macquarie University, Sydney).

1. Oppenheimer S (2009) The great arc of dispersal of modern humans: Africa to Australia. *Quat Int* 202:2–13.
2. Bräuer G (2008) The origin of modern anatomy: By speciation or intraspecific evolution? *Evol Anthropol* 17:22–37.
3. Wu XZ, Poirier FE (1995) *Human Evolution in China* (Oxford Univ Press, New York).
4. Shen G, et al. (2002) U-Series dating of Liujiang hominid site in Guangxi, Southern China. *J Hum Evol* 43:817–829.
5. Norton CJ, Jin JHJ (2009) The evolution of modern human behavior in East Asia: Current perspectives. *Evol Anthropol* 18:247–260.
6. O'Connor S (2007) New evidence from East Timor contributes to our understanding of earliest modern human colonisation east of the Sunda Shelf. *Antiquity* 81:523–535.
7. Armitage SJ, et al. (2011) The southern route "out of Africa": Evidence for an early expansion of modern humans into Arabia *Science* 331:453–456.
8. Mellars P (2006) Going east: New genetic and archaeological perspectives on the modern human colonization of Eurasia. *Science* 313:796–800.
9. Endicott P, Ho SYW, Metspalu M, Stringer C (2009) Evaluating the mitochondrial timescale of human evolution. *Trends Ecol Evol* 24:515–521.
10. Stanyon R, Sazzini M, Luiselli D (2009) Timing the first human migration into eastern Asia. *J Biol* 8:18.
11. Stoneking M, Delfin F (2010) The human genetic history of East Asia: Weaving a complex tapestry. *Curr Biol* 20:R188–R193.
12. Woo JK, Peng RC (1959) Fossil human skull of early paleoanthropic stage found at Mapa, Shaoquan, Kwantung Province. *Vertebrat Palasiatic* 3:176–182.
13. Yuan S, Chen T, Gao S (1986) Uranium series chronological sequence of some Paleolithic sites in south China. Acta Anthropolog Sinica 5:179–190.
14. Gao B, Shen GJ, Qui LC (2007) Preliminary U-series dating of southern branch cave of Maba hominid site. *J Jinan Univ* 28:308–311.
15. Liu W, et al. (2010) Human remains from Zhirendong, South China, and modern human emergence in East Asia. *Proc Natl Acad Sci USA* 107:19201–19206.
16. Shang H, Tong HW, Zhang SQ, Chen FY, Trinkaus E (2007) An early modern human from Tianyuan Cave, Zhoukoudian, China. *Proc Natl Acad Sci USA* 104:6573–6578.
17. Shang H, Trinkaus E (2010) *The Early Modern Human from Tianyuan Cave, China* (Texas A&M University, College Station, TX).
18. Guanjun S, Wei W, Hai C, Edwards RL (2007) Mass spectrometric U-series dating of Laibin hominid site in Guangxi, southern China. *J Arch Sci* 34:2109–2114.
19. Barker G, et al. (2007) The 'human revolution' in lowland tropical Southeast Asia: The antiquity and behavior of anatomically modern humans at Niah Cave (Sarawak, Borneo) *J Hum Evol* 52:243–261.
20. Woo J (1958) Fossil human parietal bone and femur from Ordos, Inner Mongolia. *Vertebrat Palasiatic* 2:208–212.
21. Woo J (1959) Human fossils found in Liukiang, Kwangsi, China. *Vertebrat Palasiatic* 3: 109–118.
22. Woo J (1959) Liukiang Man—earliest representative of modern man in East Asia. *Sci Rec* 3:165–167.
23. Détroit F, et al. (2004) Upper Pleistocene *Homo sapiens* from the Tabon cave (Palawan, The Philippines): Description and dating of new discoveries. *C R Palevol* 3:705–712.
24. Bowler JM, et al. (2003) New ages for human occupation and climatic change at Lake Mungo, Australia. *Nature* 421:837–840.
25. Kennedy KAR, Deraniyagala SU, Roertgen WJ, Chiment J, Disotell TR (1987) Upper pleistocene fossil hominids from Sri Lanka. *Am J Phys Anthropol* 72:441–461.
26. Kennedy KAR (1999) Paleoanthropology of South Asia. *Evol Anthropol* 8:165–185.
27. Curnoe D, et al. (2012) Human remains from the Pleistocene-Holocene transition of southwest China suggest a complex evolutionary history for East Asians. *PLoS ONE* 7:e31918.
28. Demeter F (2006) *Bioarchaeology of Southeast Asia. Cambridge Studies in Biological and Evolutionary Anthropology*, eds Tayles N, Oxenham M (Cambridge Univ Press, Cambridge, UK), Vol 43, pp 112–133.
29. Aitken MJ (1998) *An Introduction to Optical Dating* (Oxford Univ Press, Oxford).
30. Duller GAT (2004) Luminescence dating of Quaternary sediments: Recent advances. *J Quat Sci* 19:183–192.
31. Rink WJ, Rendell H, Marseglia EA, Luff BJ, Townsend PD (1993) Thermoluminescence spectra of igneous quartz and hydrothermal vein quartz. *Phys Chem Miner* 20:353–361.
32. Kuhn R, et al. (2000) A study of thermoluminescence emission spectra and optical stimulation spectra of quartz from different provenances. *Radiat Meas* 32:653–657.
33. Tan K, et al. (2009) Three-dimensional thermoluminescence spectra of different origin quartz from Altay Orogenic belt, Xinjiang, China. *Radiat Meas* 44:529–533.
34. Gotze J (2009) Chemistry, textures and physical properties of quartz—geological interpretation and technical application. *Mineral Mag* 73:645–671.
35. Fattahi M, Stokes S (2000) Red thermoluminescence (RTL) in volcanic quartz: Development of a high sensitivity detection system and some preliminary findings. *Ancient TL* 18:35–55.
36. Scholefield RB, Prescott JR (1999) The red thermoluminescence of quartz: 3-D spectral measurements. *Radiat Meas* 30:83–95.
37. Sládek V, Trinkaus E, Sefcáková A, Halouzka R (2002) Morphological affinities of the Sal'a 1 frontal bone *J Hum Evol* 43:787–815.
38. Heim JL (1976) Les hommes fossiles de la Ferrassie. *Archives de l'Institut de Paléontologie Humaine* (Masson et Cie, Paris).
39. Doboş A, Soficaru A, Trinkaus E (2010) The prehistory and paleontology of the Peştera Muierii, Romania. *Etud Rech Archeol Univ Liège* 124:1–122.
40. Hublin J-J (1978) Anatomie du centre de l'ecaille de l'occipital. *Cahiers d'Anthropologie (Paris)* 2:65–83.
41. Arsuaga JL, et al. (2002) The Gravettian occipital bone from the site of Malladetes (Barx, Valencia, Spain). *J Hum Evol* 43:381–393.
42. Weidenreich F (1943) The skull of Sinanthropus pekinensis: A comparative study on a primitive hominid skull. *Palaeontologia Sinica* 10D:1–485.
43. Vallois HV (1969) Le temporal néandertalien H27 de La Quina. Etude Anthropologique. *Anthropologie* 73:365–400.
44. Condemi S (1988) Caractères plésiomorphes et apomorphes de l'os temporal des néandertaliens européens würmiens. *Etud Rech Archeol Univ Liege* 30:49–52.
45. Franciscus RG (2003) Internal nasal floor configuration in *Homo* with special reference to the evolution of Neandertal facial form. *J Hum Evol* 44:701–729.
46. Wu X, Maddux S, Pan L, Trinkaus E Nasal floor variation among eastern Eurasian Pleistocene *Homo*. *Anthropol Sci*, in press.
47. Bailey S (2006) Beyond shovel-shaped incisors: Neandertal dental morphology in a comparative context. *Period Biol* 108:253–267.
48. Bailey SE, Liu W (2010) A comparative dental metrical and morphological analysis of a Middle Pleistocene hominin maxilla from Chaoxian (Chaohu), China. *Quat Int* 211: 14–23.
49. Trinkaus E (2006) Modern human versus Neandertal evolutionary distinctiveness. *Curr Anthropol* 47:597–620.
50. Stefan VH, Trinkaus E (1998) Discrete trait and dental morphometric affinities of the Tabun 2 mandible. *J Hum Evol* 34:443–468.
51. Abdulla MA, et al.; HUGO Pan-Asian SNP Consortium; Indian Genome Variation Consortium (2009) Mapping human genetic diversity in Asia. *Science* 326:1541–1545.
52. Ke Y, et al. (2001) African origin of modern humans in East Asia: A tale of 12,000 Y chromosomes. *Science* 292:1151–1153.
53. Kong QP, et al. (2011) Large-scale mtDNA screening reveals a surprising matrilineal complexity in east Asia and its implications to the peopling of the region. *Mol Biol Evol* 28:513–522.
54. Macaulay V, et al. (2005) Single, rapid coastal settlement of Asia revealed by analysis of complete mitochondrial genomes. *Science* 308:1034–1036.
55. Jin L, Su B (2000) Natives or immigrants: modern human origin in east Asia. *Nat Rev Genet* 1:126–133.